

Building block modeling technique: Application to ternary chalcogenide glasses g-Ge₂As₄Se₄ and g-AsGe_{0.8}Se_{0.8}

B. Cai

Department of Physics and Astronomy, Ohio University, Athens, Ohio 45701, USA

X. Zhang

Department of Radiation Physics, University of Texas, MD Anderson Cancer Center, Houston, Texas 77030, USA

D. A. Drabold

Department of Physics and Astronomy, Ohio University, Athens, Ohio 45701, USA

(Received 16 November 2010; revised manuscript received 7 February 2011; published 21 March 2011)

For some glasses, there are fundamental units, “building blocks” (BBs), that exist in both the liquid and glassy phases. In this Brief Report, we introduce a systematic modeling technique based on the concept of BBs and obtain *ab initio* models of g-Ge₂As₄Se₄ and g-AsGe_{0.8}Se_{0.8}. The total radial distribution function of g-Ge₂As₄Se₄ shows pleasing agreement with experimental data. The partial pair-correlation functions are predicted for both g-Ge₂As₄Se₄ and g-AsGe_{0.8}Se_{0.8}. The coordination statistics indicate that the “8-N” rule is often violated in these two ternary chalcogenide glasses. The electronic density of states with inverse participation ratio analysis is also reported.

DOI: [10.1103/PhysRevB.83.092202](https://doi.org/10.1103/PhysRevB.83.092202)

PACS number(s): 61.43.Bn, 61.43.Fs, 61.43.Dq

Owing to promising optoelectronic and electronic features,^{1–3} chalcogenide glasses have drawn extensive attention during the last decade. However, the lack of translational periodicity makes it hard to predict the microscopic structure of these glasses. Experimental results indicate that chemical order is broken and homopolar bonds are observed in chalcogenide glasses.^{4–6} To further understand the topology and its role in determining optoelectronic and electronic properties, realistic atomistic models of these glasses are required. One possible way to obtain atomic models for glasses is the standard molecular dynamic (MD) “melt and quench” method. This method seems to work when there are fundamental units existing in both liquid and glass. For simple building blocks (BBs) (involving only a few atoms), realistic models are obtained after a long liquid equilibration and a slow quench procedure. However, if the BBs are complex, such as the case in ternary alloys, it sometimes happens that the melt and quench method fails to obtain the correct structure due to the limitation of short simulation times. If *a priori* information (such as chemical order, correct coordination number, etc.) is unknown for a target material, the melt and quench technique usually starts with random initial configurations and the calculations may be extremely time consuming for large systems. Also, very large cells may be required if the structural order is complex. Our earlier studies indicated that the melt and quench method has difficulties in generating realistic atomic models of Ge-As-Se glasses (more details are discussed in Ref. 7). Thus, in this case, it is of interest to develop a new modeling technique.

Since BBs play important roles in the melt and quench method, we may first attempt to generate energetically reasonable (energy is minimum) BBs and then build a large cell from those BBs. This idea is based on two assumptions: (1) No dramatic changes in local order occur between the large system and the small system; (2) BBs exist in these glasses and the correct chemical order can be obtained by a long *ab*

initio molecular-dynamics simulation.^{7,8} In this Brief Report, we describe a systematic modeling technique to obtain BBs and then to achieve big models. By applying this method, we construct *ab initio* models of g-Ge₂As₄Se₄ and g-AsGe_{0.8}Se_{0.8}. We compare the radial distribution function of g-Ge₂As₄Se₄ with experimental data and predict the partial pair-correlation function for both g-Ge₂As₄Se₄ and g-AsGe_{0.8}Se_{0.8}. The electronic structures are studied through the electronic density of states. We found a 0.34-eV and a 0.38-eV electronic band gap for g-Ge₂As₄Se₄ and g-AsGe_{0.8}Se_{0.8} within the local-density approximation (LDA).

We start our discussion by describing the MD procedures that are used to generate the atomic models. A flowchart to illustrate this method is given in Fig. 1. A small number of atoms are randomly placed into a cubic box, which we named as the subunit cell, with the correct stoichiometry and experimental mass density. For g-Ge₂As₄Se₄, 25 atoms (5 Ge, 10 Se, and 10 As) are in each subunit cell with mass density 4.687 g/cm³ (lattice constant is 8.75 Å). For g-AsGe_{0.8}Se_{0.8}, 26 atoms (8 Ge, 10 As, and 8 Se) are in each subunit cell with mass density 4.459 g/cm³ (lattice constant is 9 Å). The subunit cells are then melted at 5000 K for 1 ps, equilibrated at 2000 K for 15 ps, cooled over 1000 K for 15 ps, annealed to 300 K for 15 ps, and quenched to 0 K. These steps are repeated on the same subunits for several cycles, until the minimum-energy structures are unchanged. At this point, energetically optimized BBs are obtained. Then large unit cells are built from these BBs (200 atoms cells for g-Ge₂As₄Se₄ and 208 atoms cell for g-AsGe_{0.8}Se_{0.8}). We fix the temperature in the large cells at 1500 K (above the melting point) for 7.5 ps, anneal to 300 K, and quench to 0K.⁷ All the MD steps are done via the density-functional quantum molecular-dynamics method FIREBALL96 with local basis sets.⁹ To further improve the chemical order and eliminate artifacts of the minimal basis, we annealed our models at 300 K for 5 ps and quench to 0 K with the Vienna Ab-initio Simulation Package (VASP)¹⁰—a

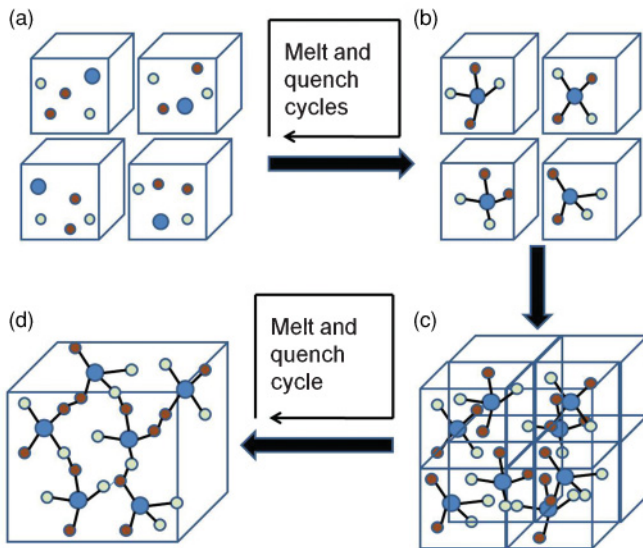


FIG. 1. (Color online) Flowchart for building block modeling method. (a) Atoms in subunits cell with random initial positions. (b) Building blocks (BBs) are obtained after several melt and quench cycles with unchanged minimum energy. (c) A large cell built, based on BBs. (d) Final models are obtained after one melt, quench/anneal cycle.

plane-wave density-functional theory (DFT) code using the local-density approximation (LDA). The final models are obtained after an energy relaxation. In all calculations, only the Γ point is used to sample the Brillouin zone. The electronic density of states (EDOS) is calculated with VASP.

The final models are shown in Fig. 2. We emphasize that there are no remaining correlations between the subunit cells in our final models. For $g\text{-Ge}_2\text{As}_4\text{Se}_4$, the radial distribution functions (RDFs) and partial pair-correlation functions (PPCFs) are shown in Fig. 3. The calculated total RDF indicates a sharp first peak at 2.47 Å, a first minimum at 2.81 Å, and a broad second peak around 3.7 Å. All the peak positions agree with experimental data from Ref. 11, which implies that the building block techniques manage to obtain not only the correct local structure order but also a reasonable medium-range order. The partial pair-correlation functions for $g\text{-Ge}_2\text{As}_4\text{Se}_4$ are plotted in Fig. 3(b). Ge-Se, As-Se, Ge-As, and As-As all have a strong first peak around 2.5 Å which collectively produce the first peak in the total RDF. Se-Se homopolar bonds are not observed in our models. We also noticed that As atoms bond with both

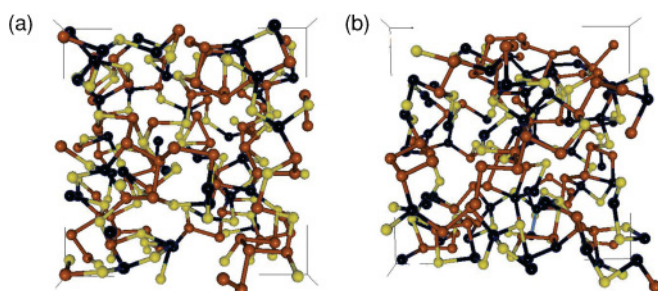


FIG. 2. (Color online) Atomic models for (a) 200-atom $g\text{-Ge}_2\text{As}_4\text{Se}_4$ and (b) 208-atom $g\text{-AsGe}_{0.8}\text{Se}_{0.8}$. Black (dark) atoms are Ge, brown (gray) atoms are As, green (light) atoms are Se.

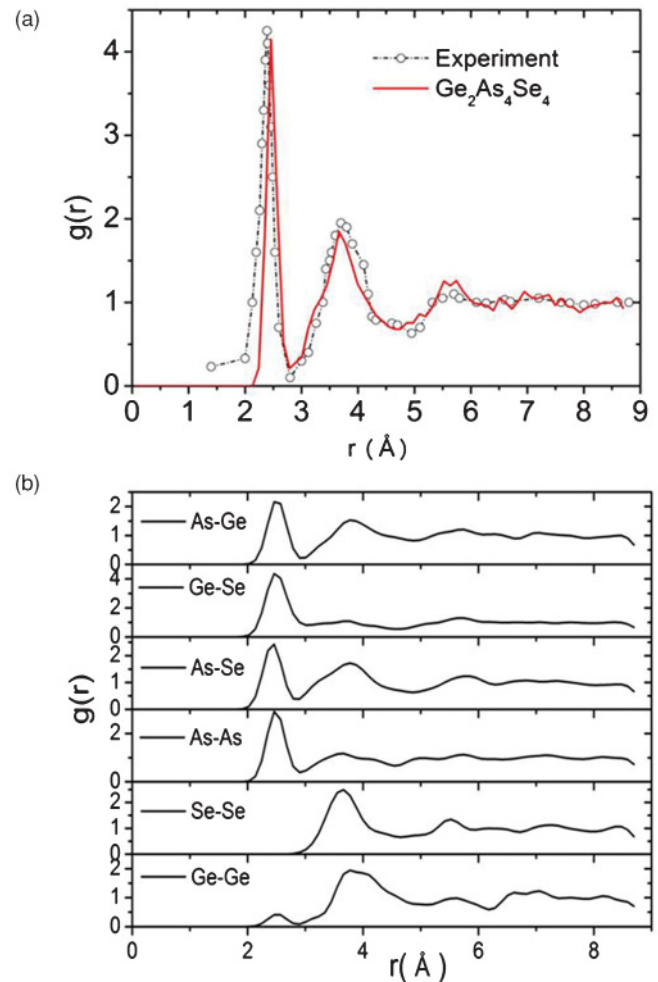


FIG. 3. (Color online) Radial distributions and partial pair-correlation functions of $g\text{-Ge}_2\text{As}_4\text{Se}_4$. Experimental data are from Ref. 11.

Ge and Se atoms, which does not support the assumption that As-Ge bonds have low formation probability.¹² We list the averaged bond distance in Table I and they are close to the value predicted in Ref. 11. Notice that Ref. 11 predicted 2.41 Å for the As-As bond, which is 3% lower than the standard value [2.49 Å for amorphous As¹³ and 2.51 Å in rhombohedral As (Ref. 14)], our results are actually closer to the standard value. For $g\text{-AsGe}_{0.8}\text{Se}_{0.8}$, the total RDF shows similar features to $g\text{-Ge}_2\text{As}_4\text{Se}_4$. With an increased concentration of Ge atoms, As-Se partial exhibits a weak first peak and a strong second

TABLE I. Mean bond length in $g\text{-Ge}_2\text{As}_4\text{Se}_4$ and comparison with Ref. 11.

Bond type	Distance (Å)	Ref. 11 (Å)
Ge-Ge	2.47	2.51 ± 0.19
Ge-As	2.53	2.44 ± 0.14
Ge-Se	2.53	2.48 ± 0.15
As-As	2.50	2.41 ± 0.07
As-Se	2.44	2.41 ± 0.06

TABLE II. Coordination numbers and bond-type analysis of computer generated g-Ge₂As₄Se₄ and g-AsGe_{0.8}Se_{0.8}.

Alloys	Element	Coordination				Mean	Bond type		
		5	4	3	2		Ge%	As%	Se%
g-Ge ₂ As ₄ Se ₄	Ge	4	20	16	0	3.7	3	30	67
	As	0	6	74	0	3.1	18	45	37
	Se	0	1	30	49	2.4	52	48	0
g-AsGe _{0.8} Se _{0.8}	Ge	1	37	26	0	3.6	14	34	52
	As	0	8	70	2	3.1	32	49	19
	Se	0	0	39	25	2.6	72	28	0

peak; the number of Ge-Ge bonds is also increased. Again, Se-Se bonds are not observed.

The structural statistics for coordination and chemical order are computed for both models, and we report the result in Table II. One observation is that the 8-N rule is not valid for our models. For g-Ge₂As₄Se₄, the majority of Ge, As, and Se are fourfold, threefold, and twofold, respectively. However, there is a significant fraction of threefold Ge atoms and threefold Se atoms in the system. For g-AsGe_{0.8}Se_{0.8}, the majority of Ge atoms are still fourfold and As atoms remain threefold, while *most* Se atoms are threefold. This may be due to a relatively large concentration of Ge atoms (compared with g-Ge₂As₄Se₄) and implies that g-AsGe_{0.8}Se_{0.8} has a more rigid three-dimensional network. These undercoordinated Ge atoms and overcoordinated Se atoms do not introduce midgap states or highly localized tail states, so we do not interpret them as a defect. The average coordination $\langle r \rangle$ of our model is 2.93 for g-Ge₂As₄Se₄ and 3.08 for g-AsGe_{0.8}Se_{0.8}, which is different from the standard values proposed by Thorpe and Phillips (2.8 for g-Ge₂As₄Se₄ and 3.0 for g-AsGe_{0.8}Se_{0.8}) based on 8-N constraints^{15,16} (where the averaged coordination $\langle r \rangle$ is calculated as $\langle r \rangle = 4X_{Ge} + 3X_{As} + 2X_{Se}$. X_{Ge} , X_{As} , and X_{Se} are the concentration of Ge, As, and Se atoms). When $\langle r \rangle$ is bigger than 2.8, it is believed that Ge-As-Se alloys form a three-dimensional rigid network due to the vulcanization or *cross linking*. The difference here may imply that the constraint counting of Ge-As-Se alloys in this cross-linked three-dimensional (3D) region should be carefully reconsidered. Violations of the 8-N rule are well known in other chalcogenide systems.¹⁷

Without any *a priori* information, the building-block method provided us reasonable models of g-Ge₂As₄Se₄ and g-AsGe_{0.8}Se_{0.8}. We should be clear that the building-block technique is not new in modeling disordered materials. Amorphous Si₃N₄ models were made by Ouyang and co-authors through assembling a small number of fundamental building blocks.¹⁸ However, the building blocks in our method were built purely from first-principles calculation and the recipe is, in principle, perfectly general. Moreover, the final melt and quench cycle for the large cell managed to maintain correct short-range order, destroy the correlation of BBs, and obtain credible medium-range order at the same time. Considering the efficiency, since the large cells are constructed based on reasonable BBs, our simulation has a shorter computation time compared to the traditional method searching for optimum structures from random initials.

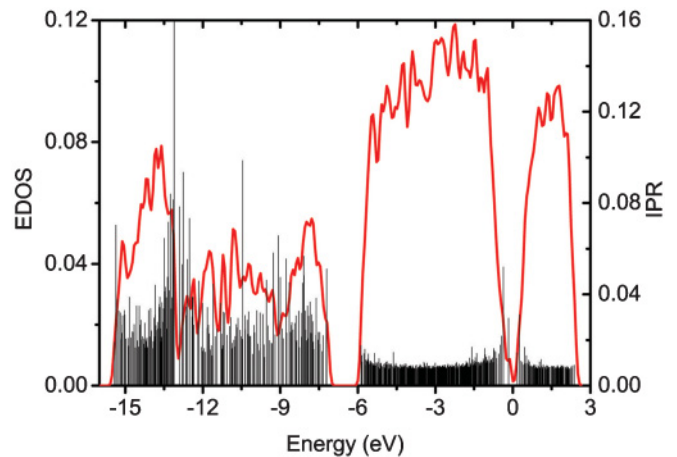


FIG. 4. (Color online) Electronic density of states (EDOS) and inverse participation ratio (IPR) for g-Ge₂As₄Se₄ model. The Fermi level is at 0 eV.

The electronic structure was analyzed through electronic density of states (EDOS) and inverse participation ratio (IPR). The IPR measures the localization for each eigenstate. For ideally localized states, $IPR = 1$; for extended states, $IPR = N^{-1}$, where N is the number of atoms. (Details are discussed in Ref. 19. All calculations are done via VASP.) The EDOS of g-Ge₂As₄Se₄ in Fig. 4 indicates a 0.34-eV band gap and a midgap state. High IPR states are observed in the region from -15.5 eV to -6.5 eV and around the valence- and conduction-band edge. We then studied the localization by projecting the density of states onto different species. We could see from Fig. 5 that Se atoms contribute to the region from -15.5 eV to -13 eV, As atoms contribute to the region from -12.9 eV to -8.6 eV, and Ge atoms contribute to the region from -8.6 eV to -7.2 eV. The eigenstates in the region from -5 eV to -1 eV are quite extended. The valence-band tail states and conduction-band tail states tend to be localized on As and Ge atoms. A further investigation shows that the gap states are mainly localized on overcoordinated (fivefold) Ge atoms and its neighbors. The valence tail state with highest IPR

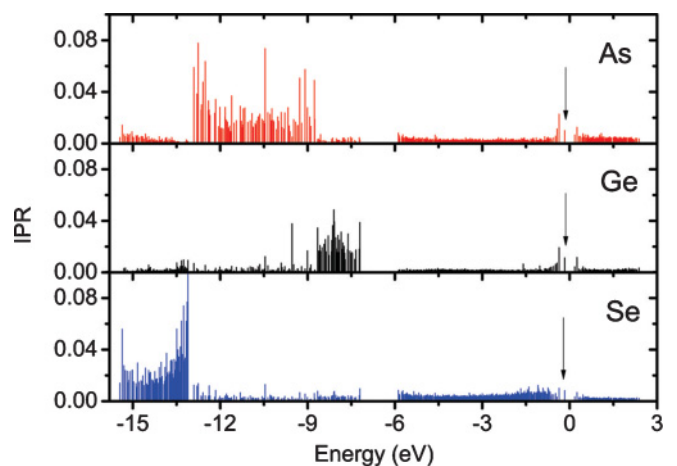


FIG. 5. (Color online) Projected IPR for g-Ge₂As₄Se₄ according to different species. The midgap state is marked by black arrow. The Fermi level is at 0 eV.

is localized on a distorted site where three atoms (1 Ge, 1 As, and 1 Se) form a triangle. We believe that the overcoordinated Ge site and the distorted triangle site would be eliminated through an extended annealing. The DOS of $g\text{-AsGe}_{0.8}\text{Se}_{0.8}$ exhibits a similar shape to $g\text{-AsGe}_{0.8}\text{Se}_{0.8}$ but with a 0.38-eV band gap and no midgap states. As atoms highly contribute to the valence- and conduction-band tail states. We should point out here that undercoordinated (threefold) Ge atoms and overcoordinated (threefold) Se atoms do not introduce localized states or midgap states, especially in $g\text{-AsGe}_{0.8}\text{Se}_{0.8}$ where most Se are threefold, which implies that they are not defects in the network. It is well known that the LDA method always underestimates the magnitude of the band gap, so other techniques could be applied to get a better prediction for the band gap.¹⁷

To sum up, we introduced a BB modeling technique and applied it to obtain atomic models of $g\text{-Ge}_2\text{As}_4\text{Se}_4$

and $g\text{-AsGe}_{0.8}\text{Se}_{0.8}$. Both models predict reasonable RDFs and PPCFs, and the RDF of $g\text{-Ge}_2\text{As}_4\text{Se}_4$ shows reasonable agreement with experimental data. A significant fraction of overcoordinated Ge and undercoordinated Se are found in the system without introducing defect states in electronic structure, and we believe that these undercoordinated (threefold) Ge and overcoordinated Se (threefold) are not defects. This result may imply that the 8-N rule is violated and the coordination constraint counting should be reconsidered in the rigid network region of Ge-As-Se alloys. We found a 0.34-eV band gap with a midgap state for $g\text{-Ge}_2\text{As}_4\text{Se}_4$ and a 0.38-eV band gap for $g\text{-AsGe}_{0.8}\text{Se}_{0.8}$, which could be well underestimated by the LDA method.

This work was supported by US NSF Grant No. DMR 09-03225.

¹R. W. Haisty and K. Krebs, *J. Non-Cryst. Solids* **1**, 427 (1969).

²P. J. Webber and J. A. Savage, *J. Non-Cryst. Solids* **20**, 271 (1976).

³T. T. Nang, M. Okuda, and T. Matsushita, *Phys. Rev. B* **19**, 947 (1979).

⁴I. Petri, P. S. Salmon, and H. E. Fischer, *Phys. Rev. Lett.* **84**, 2413 (2000).

⁵P. Hari, P. C. Taylor, W. A. King, and W. C. LaCourse, *J. Non-Cryst. Solids* **198**, 736 (1996).

⁶P. S. Salmon, A. C. Barnes, R. A. Martin, and G. J. Cuello, *Phys. Rev. Lett.* **96**, 235502 (2006).

⁷X. Zhang, Ph.D. Thesis, Ohio University, Athens, 2001.

⁸D. A. Drabold, *Eur. Phys. J. B* **68**, 1 (2009).

⁹O. F. Sankey and D. J. Niklewski, *Phys. Rev. B* **40**, 3979 (1989); J. P. Lewis, K. R. Glaesemann, G. A. Voth, J. Fritsch, A. A. Demkov, J. Ortega, and O. F. Sankey, *ibid.* **64**, 195103 (2001); [<http://www.fireball-dft.org/web/fireballHome>].

¹⁰G. Kresse and J. Furthmuller, *Phys. Rev. B* **54**, 1116 (1996); [<http://cmp.univie.ac.at/vasp/>].

¹¹N. de la Rosa-Fox, L. Esquivias, P. Villares, and R. Jimenez-Garay, *Phys. Rev. B* **33**, 4094 (1986).

¹²Z. U. Borisova, *Glassy Semiconductors* (Plenum, New York, 1981).

¹³G. N. Greaves and E. A. Davis, *Philos. Mag.* **29**, 1201 (1974).

¹⁴X. Wyckoff, in *Crystal Structure* (Wiley, New York, 1963).

¹⁵J. C. Phillips, *J. Non-Cryst. Solids* **34**, 153 (1979).

¹⁶M. F. Thorpe, *J. Non-Cryst. Solids* **57**, 355 (1983).

¹⁷B. Cai, D. A. Drabold, and S. R. Elliott, *Appl. Phys. Lett.* **97**, 191908 (2010).

¹⁸L. Ouyang and W. Y. Ching, *Phys. Rev. B* **54**, 15594 (1996).

¹⁹D. A. Drabold, P. A. Fedders, Stefan Klemm, and O. F. Sankey, *Phys. Rev. Lett.* **67**, 2179 (1991); D. A. Drabold and P. A. Fedders, *Phys. Rev. B* **60**, 721 (1999); D. A. Drabold, *J. Non-Cryst. Solids* **266**, 211 (2000); Raymond Atta-Fynn, Parthapratim Biswas, and D. A. Drabold, *Phys. Rev. B* **69**, 245204 (2004).